Proceedings of the International Conference
Preventive and Planned Conservation
Monza, Mantova - 5-9 May 2014

I contributi presentati al convegno restituiscono un'articolata panoramica di riflessioni e di casi studio, in cui emerge come filo conduttore la capacità di esprimere una visione di lungo periodo e di proporre una virtuosa integrazione fra strategie, spesso innovative, di conservazione e di valorizzazione.

PPC Conference 2014 è una delle attività di comunicazione e divulgazione previste dell'ambito dei Distretti Culturali "Monza e Brianza" e "Le Regge dei Gonzaga", esperienze che testimoniano come il patrimonio storico architettonico costruito possa ricoprire un ruolo nuovo e determinante nelle dinamiche di sviluppo locale.

I volumi:

1 La strategia della Conservazione programmata.
Dalla progettazione delle attività alla valutazione degli impatti.

2 Sguardi ed esperienze sulla conservazione del patrimonio storico architettonico.

3 Protezione dal rischio sismico.

4 Metodi e strumenti per la prevenzione e manutenzione.

5 ICT per il miglioramento del processo conservativo.

A cura di **Stefano Della Torre**
Curatela editoriale **Maria Paola Borgarino**

ISBN 978-88-404-0316-8
€ 25,00

Protezione dal rischio sismico

NARDINI EDITORE

Proceedings of the International Conference
Preventive and Planned Conservation
Monza, Mantova - 5-9 May 2014

3

Protezione dal rischio sismico

A cura di **Stefano Della Torre**
Curatela editoriale **Maria Paola Borgarino**

NARDINI EDITORE

Proceedings of the International Conference
Preventive and Planned Conservation
Monza, Mantova - 5-9 May 2014

Protezione dal rischio sismico

Proceedings of the International Conference
Preventive and Planned Conservation
Monza, Mantova - 5-9 May 2014

Comitato scientifico
Carlo Blasi, *Università di Parma, Italy*
Federico Bucci, *Politecnico di Milano, Italy*
Fausto Cardoso Martinez, *University of Cuenca, Ecuador*
Angelo Ciribini, *Università di Brescia, Italy*
Nigel Dann, *University of the West of England, United Kingdom*
Stefano Della Torre, *Politecnico di Milano, Italy*
Sasa Dobrĭčĭč, *University of Nova Gorica, Slovenia*
Xavier Greffe, *Université Paris 1 Panthéon-Sorbonne, France*
Massimo Montella, *Università di Macerata, Italy*
Elena Mussinelli, *Politecnico di Milano, Italy*
Christian Ost, *ICHEC Brussels Management School, Belgium*
Ana Pereira Roders, *University of Eindhoven, Holland*
Pietro Petraroia, *Eupolis Lombardia, Italy*
Mario Santana Quintero, *Carleton University, Canada*
Koenraad Van Balen, *UNESCO Chair for PRECOMOS, KU Leuven, Belgium Minja Yang, RLICC, KU Leuven, Belgium*
Rossella Moioli, *Distretto Culturale Monza e Brianza, Italy (coordinamento)*

Segreteria scientifica del convegno:
Maria Paola Borgarino, Stefania Bossi
Politecnico di Milano, Dipartimento ABC - Architecture, Built Environment and Construction Engineering

Atti a cura di Stefano Della Torre
Curatela editoriale: Maria Paola Borgarino
Impaginazione e collaborazione alla revisione dei testi: Cristina Boniotti

Politecnico di Milano - Dipartimento ABC - Architecture, Built Environment and Construction Engineering
Fondazione Cariplo, progetto Distretti Culturali
Distretto Culturale Evoluto di Monza e Brianza - Provincia di Monza e della Brianza
Distretto Culturale Le Regge dei Gonzaga

Con il patrocinio della

RegioneLombardia

@ 2014 Politecnico di Milano e Nardini Editore
Tutti i diritti sono riservati

Copertina Ennio Bazzoni

Stampato per Nardini Editore

Proceedings of the International Conference
Preventive and Planned Conservation
Monza, Mantova - 5-9 May 2014

3

Protezione dal rischio sismico

A cura di **Stefano Della Torre**
Curatela editoriale **Maria Paola Borgarino**

NARDINI EDITORE

Indice

RETROFITTING OF MASONRY STRUCTURES WITH COMPOSITE MATERIALS. EXPERIMENTAL AND NUMERICAL RESULTS

Gaia Barbieri, Massimiliano Bocciarelli, Lorenzo Borrello, Sara Cattaneo
Politecnico di Milano, Department of Architecture, Built Environment and Construction Engineering

Abstract

In this paper, delamination phenomena between carbon fiber reinforced polymer (CFRP) strips and masonry support have been investigated on the basis of single-lap shear tests, considering different dimensions of the bonded lengths. To capture the post-peak response of the CFRP-masonry joint, the slip between the support and the reinforcement strip has been controlled using a clip gage at the end of the reinforcement. The experimental results have been compared with similar tests performed on concrete specimens, especially for what concern the failure mechanisms. The tests have been simulated by means of a finite element model to describe the mechanism involved in the failure process. The numerical model considers a zero-thickness interface elements and a proper non-linear cohesive law. The comparison between experimental and numerical results has been performed in terms of maximum force and pre-peak response of the CFRP-masonry joint, considering the case of effective bonded length greater or lesser than the minimum anchorage length suggested by the CNR Italian recommendation.

A significant portion of the world heritage buildings is constituted by unreinforced masonry structures particularly susceptible to damage from accidental loads. In the last decades, the need to strengthen these structures has induced the development of strengthening techniques based on the use of composite materials. Among these, one of the most commonly used technique is represented by FRP strips which can be externally glued on both the concrete and masonry substrates. FRP materials present several advantages that allow them to be particularly suitable for civil constructions reparation and rehabilitation. However, some concern exists on the bond between the composite material and the substrate.

In recent years, several experimental and numerical investigations have been conducted for concrete structure reinforced by FRP systems (Nakaba, 2001; Monti, 2003; Lu, 2005; Ferracuti, 2007), but only in the last few years

some study have been carried out with reference to masonry supports (Aiello, 2006; Panizza, 2008; Grande, 2011; Ghiassi, 2012; Ceroni, 2014).

In this paper, the problem of the bond strength in a "pull" test on three masonry specimens with different bonded lengths of the strips was examined. Single-lap shear tests initially controlled by the load edge displacement and subsequently, at the onset of the debonding process, by a clip gage mounted at the end of the reinforcement, are presented. In this way, the complete equilibrium paths were followed up to debonding of the reinforcement from the masonry support, independently from the bonded length. The experimental results showed some similarities with the results on concrete specimens, but also some differences, mainly owing to the greater heterogeneity of the material. In particular, the concern regarded the creation of a resistant bulb and of two mechanisms of failure in competition during the progressive damage and crackers formation of strengthen masonry specimens. Moreover, according to what suggested by the Italian recommendation (CNR DT200, 2013), the existence of a minimum length was established, past which the ultimate load cannot further increase.

The numerical simulations of the tests allowed to investigate the failure modes and to demonstrate the influence of the effective bonded length on the ultimate load. To this purpose, it was crucial to correctly estimate the interface behavior between masonry and CFRP.

In the analyzed cases, an exponential cohesive law used in (Bocciarelli, 2012) for steel specimens reinforced using CFRP plates was selected, resuming the one originally proposed in (Ortiz, 1999). In this model was used a zero-thickness interface elements between the FRP and the substrate. The non-linearities have been concentrated at this interface, while FRP and substrate were characterized by an elastic behavior.

By means of a best fitting procedure, performed starting from input data calculated on the basis of the Italian recommendation (CNR DT200, 2013), the assumed law allowed to reach a good agreement between the experimental and numerical results, compared in terms of ultimate load and pre-peak response of the CFRP-masonry joint, in particular for what concerns the stiffness.

Experimental techniques

Specimens preparation and mechanical properties of the materials

Three prismatic masonry specimens were constituted by standard bricks, with size 250 x 120 x 55 mm, intersected by fiber-reinforced cement mortar joints with thickness 20 mm.

The mechanical properties of brick and mortar are reported in Tab. 1. The tests on mortar specimens were conducted at 90 days of curing, just before the test on masonry pillars.

The material properties of the 0,10 mm thick carbon fiber reinforced polymer (CFRP), externally glued to the substrate by an *in situ* impregnation with an epoxy resin, were: tensile strength equal to 4,8 GPa, Young modulus equal to 215 GPa with a maximum deformation of 2,2%.

The different reinforcement configurations characterized by strips 50 mm width and 50-100-150 mm bonded lengths were tested.

	Mortar	Brick
Compressive strength fc (MPa)	45	14
Tensile strength ft (MPa)	6,0	0,7
Young modulus E (GPa)	15,0	2,4
Poisson's ratio ν	0,10	0,15

Tab. 1 - Brick and mortar properties.

Experimental setup

The testing system consisted of a closed-loop electromechanical Instron load frame with a maximum capacity of 100 kN (Fig. 1).

The specimen was fixed by means of a steel support designed to reduce the elastic rotation. The supporting steel plates were controlled by bolts, which permitted reduction in geometrical eccentricities by regulating the specimen arrangement. The end of the FRP strip subjected to traction was clamped within two steel plates compressed by bolts. To capture the post-peak behavior of the system and the softening branch in the load displacement curve, the tests were performed in a servo-controlled load frame, with a strain gauge transducer (clip gauge) that measured the relative slip between the FRP strip at the end of the reinforcement and the substrate as the feedback signal. In addition, two LVDTs measured the relative displacements of the FRP strip at the beginning of the bonded area and the substrate.

The tests were started in stroke control until the displacement measured by the clip gauge registered some displacements; then the control was switched to the clip gauge.

Experimental results

The brittle response of the joints is shown in Fig. 2. In Fig. 2a, the load-stroke curves present post peak snap-back branches and only with the adopted feedback signal was possible to follow the post-failure range. Fig. 2b shows the different load-clip gauge displacement curves for different bonded lengths.

In Tab. 2 the results of these experimental tests are summarized and compared to the theoretical predictions based on the design formula suggested in CNR DT200 (CNR DT200, 2013).

According to this recommendation, the specific fracture energy Γ_F can be evaluated as:

$$\Gamma_F = k_g k_b \sqrt{f_{bc} f_{bt}}, \qquad (1)$$

where k_g is an empirical coefficient (assumed equal to 0,093 mm or 0,031 mm to evaluate the mean Γ_{Fm} or characteristic value Γ_{Fk}, respectively) and k_b is a non-dimensional geometrical coefficient which is computed equal to 1,528, for the assumed geometrical configuration.

In (1), f_{bc} and f_{bt} denotes the mean value of the compressive and tensile strength of the masonry bricks, respectively. The masonry average tensile strength f_{bt} can be assumed to be equal to 10% of the average compressive strength.

The minimum bonded length l_e is defined as:

$$l_e = \frac{1}{\tau_f}\sqrt{\frac{\pi^2 E_f t_f \Gamma_F}{2}}, \qquad (2)$$

being τ_f the maximum shear stress in the interface FRP-substrate defined according to a bilinear constitutive relationship in terms of average shear stress versus tangential slip, as defined in Section 4.2. Considering Γ_{Fm} or Γ_{Fk}, the mean bonded length l_{em} or a design bonded length l_{ed} are defined, respectively.

Then, the theoretical maximum force $F_{max,th}$ transmitted by a joint with bonded length l_b equal or greater than l_e, is given by:

$$F_{max,th} = b_f \sqrt{2 E_f \Gamma_F t_f}, \qquad (3)$$

where E_f and t_f are the Young modulus and thickness of FRP strip, respectively. Considering Γ_{Fm} or Γ_{Fk}, the mean maximum force $F_{max,th,m}$ or the characteristic maximum force $F_{max,th,k}$ are assessed, respectively.

Conversely, if the effective bonded length l_b is smaller than the minimum bonded length l_e, the force $F_{max,th}$ has to be reduced to:

$$F_{max,th,rid} = F_{max,th} \frac{l_b}{l_e}\left(2 - \frac{l_b}{l_e}\right). \qquad (4)$$

The results reported in Tab. 2 show that the theoretical predictions are closer to the mean values of the experimental maximum force.

The experimental results confirmed that the maximum force increases with the bonded length, but once the minimum bonded length l_e is reached, the ultimate load cannot further increase. This means that if the minimum bonded length l_e is guaranteed (Test 2 and Test 3), the maximum force is independent on the bonded length and it depends on the fracture energy Γ_F only; if the minimum bonded length l_e is not guaranteed (Test 1), the maximum force also depends on the bonded length.

In the delamination process on strengthened concrete specimens a final competition of two damage mechanisms occur: i) debonding along the stiffener-substrate interface (mode-II), starting from the loaded end and generally affecting few millimeters from the concrete-to-adhesive surface, ii) cracking (mixed-mode) at the free end of the stiffener along an inclined path, with the formation of a resistant bulb. In general, debonding can occur when the shear contact stress is greater than the maximum allowable strength of the interface. On the other hand, the inclined crack opens when the strain energy release associated with its propagation is not lower than the corresponding fracture energy of the substrate itself. In particular, it appears that the formation of a resistant bulb allows the system to reach a higher maximum force. This phenomenon is shown by the load-stroke and load-clip curves where, after an instantaneous load drop (first peak) corresponding to the formation of the bulb, a new load increase up to reach the maximum value of failure (second peak) appears (Biolzi, 2013).

In the case of reinforced masonry specimens, the formation of the bulb did not emerge clearly and the delamination seemed to involve the cortical layer of bricks and mortar. The mechanical behavior shown in the load-stroke and load-clip curves generally presents a linear branch up to the maximum load. Only in the case of 150 mm bonded length, the curve seems to show the presence of a

first peak before reaching the maximum force, the second peak. Note that the first peak is approximately in correspondence of the maximum load achieved with a 100 mm bonded length (around 11.4 kN). Therefore, the formation of the first peak, and of a sort of bulb, could cause an increment of the joint performance with an ultimate load slightly higher than expected form the case of bonded length equal to 100 mm.

	Reinforcement	$F_{max,exp}$	l_{em}	l_{ed}	$F_{max,th,m}$	$F_{max,th,k}$
Test 1	50 mm x 50 mm	5,8 kN	78 mm	169 mm	5,3 kN	2,0 kN
Test 2	50 mm x 100 mm	11,4 kN	55 mm	96 mm	12,2 kN	7,0 kN
Test 3	50 mm x 150 mm	13,6 kN	55 mm	96 mm	12,2 kN	7,0 kN

Tab. 2 - Comparison of the maximum force: experimental and theoretical results.

Numerical analyses

Numerical modeling

The push pull test was simulated adopting plane stress finite elements using the code Abaqus. The lower edge of the numerical model was constrained in vertical direction and 3/4 of the right edge (starting from the bottom) was constrained in horizontal direction. An incremental monotonic displacement load was applied to the free end of the FRP strip. The mesh was constituted by linear quadrilateral elements. It was refined where higher stress gradients and damage and cracking phenomena were expected. Zero-thickness elements were inserted between masonry and FRP to take into account the non-linear behavior of the interface. In particular, the cohesive law at the interface was implemented in the finite element code by user's defined routine. Otherwise, FRP strip, bricks and mortar were assumed as linear, elastic materials, with the mechanical properties reported in Section 2.1.

Cohesive model

The bond-slip behavior of the joint between FRP sheet and the support, in terms of shear stress τ versus tangential slip s, can be idealized by means of a bilinear function (CNR DT200, 2013). After an initial elastic branch, the behavior is assumed quasi brittle, with a linear decrease of the bond strength until an ultimate slip s_u is reached, corresponding to a detachment of the reinforcement.

It is assumed the mean value of the adhesive tangential stress τ_f, corresponding to the peak of the function, to be equal to:

$$\tau_f = \frac{2\Gamma_{Fm}}{s_u}, \qquad (5)$$

where s_u in the case of masonry brick can be chosen equal to 0,40 mm.

If t_a is the adhesive layer thickness and t_M is the thickness of the masonry layer that takes part to the interface deformability (suggested equal to 25 mm), the elastic slope of the interface response can be derived as follow:

$$K_1 = \frac{c_1}{t_a / G_a + t_M / G_M}, \qquad (6)$$

with G_a and G_M the shear modulus of the adhesive and that of the support, respectively, and c_1=0,6. For the problem analyzed, $t_a/G_a \approx 0$, whereas the (homogenized) masonry shear modulus is estimated according to (D.M. 20/11/1987) (i.e. $G_M = 400\ f_{bc}$).

However, it is well known that the role played in the numerical simulations by the shape of the cohesive law is marginal compared to the role played by the peak of the curve and the area under it. For this reasons, the exponential cohesive law used in (Bocciarelli, 2012) was selected.

The adopted cohesive law was characterized by three independent parameters: the mode-I resistance σ_f, the mode-II resistance τ_f and the fracture energy Γ_{Fm}. As reported in Section 3., in the case of single-lap shear test here considered, the delamination process was mode-II dominant, and therefore the adopted mode-dependent cohesive law played in this case a marginal role.

Numerical and experimental results

The results of numerical model were analyzed in terms of the global response of the specimens, propagation of debonding and applied force versus displacement curves.

About of propagation of the debonding process, in all cases, the analyses pointed out that after having removed the initial part of the strip, a sufficiently small portion remained attached and at the end of the reinforcement a significant shear and normal stresses developed (Fig. 3). Such phenomenon seemed

to confirm the two different competing failure processes observed in strengthened concrete specimens.

The comparison between the numerical and experimental results was evaluated on the load-clip gage displacement curves, in terms of pre-peak behavior and average peak load.

The numerical results were obtained with best fitting procedure, changing parameters σ_f, τ_f and Γ_{Fm} starting from those suggested in (CNR DT200, 2013).

The numerical analyses demonstrated that:

- if $l_b < l_e$ (Test 1), the bonded area is not long enough to let the cohesive process zone develop completely and therefore the actual load carrying capacity is smaller than the maximum attainable force. $F_{max,th,m,rid}$ is a function of both Γ_F and τ_f (4);
- if $l_b > l_e$ (Test 2 and Test 3), the maximum force is the same as the one attained for $l_b = l_e$. In fact, as soon as the process zone is completely developed, the force cannot increase anymore and $F_{max,th,m}$ is a function of Γ_F only (3).

For 50 mm bonded length (Test 1), the calibration of the parameters Γ_F and τ_f according to Tab. 3 allowed to reach a very good agreement between the numerical and experimental results in terms of both stiffness and maximum load. The results are reported in Tab. 4 for what concerns the maximum force and in Fig. 4 for what concerns the load-clip gage displacement curve.

In the case of 100 and 150 mm bonded length specimens (Test 2 and Test 3) the calibration of the independent parameters should have given rise to similar values. However, it was possible to observe that the maximum experimental forces were well predicted by the numerical simulations after the best fitting procedure, but the stiffness of the systems were very different. Calibrating the maximum load in both the system, that mainly depends on the parameter Γ_F, the stiffness was defined by the parameter τ_f, which was consequently assessed taking into account that an excessive drop of τ_f could cause an excessive increase of the minimum bonded length and so a reduction of the ultimate load (Tabb. 3, 4 and Fig. 4).

	$\tau_{f,CNR}$	$\tau_{f,bestfit}$	$\frac{\tau_{f,bestfit}}{\tau_{f,CNR}}$	$\Gamma_{Fm,CNR}$	$\Gamma_{Fm,bestfit}$	$\frac{\Gamma_{Fm,bestfit}}{\Gamma_{Fm,CNR}}$
	[MPa]	[MPa]		[N/mm]	[N/mm]	
Test 1	2,78	3,34	1,20	0,45	0,40	0,90

Test 2	6,91	8,98	1,30	1,38	1,38	1,00
Test 3	6,91	2,76	0,40	1,38	1,38	1,00

Tab. 3 - Comparison between the parameters τ_f and Γ_{Fm} as suggested by the recommendation and as adopted for the best-fitting curve.

	$F_{max,exp}$	$F_{max,num}$	Err.
Test 1	5,8 kN	5,9 kN	1,7 %
Test 2	11,4 kN	11,9 kN	4,4 %
Test 3	13,6 kN	11,6 kN	17,2 %

Tab. 4 - Comparison between the maximum force in the experimental and numerical analyses.

Conclusion

Delamination phenomena between a carbon fiber reinforced polymer strip and a masonry substrate were investigated by means of single-lap share specimens with different bonded lengths. To monitor the complete failure process, the tests were conducted with a clip gauge located at the free end of the strip as feedback signal to the servo-controller. It was not experimentally detected the formation of a resistant bulb inside the bulk material at the end of the reinforcement, as well as was clearly emerged on concrete specimens. However, the numerical simulations showed that the debonding process was dominated by a mode-II cracking, but at the end of the reinforcement a mix-mode cracking arose. This confirmed the presence of two different competing failure processes even in the case of masonry specimens.

The adopted finite element model was validated on the basis of the comparison of the Italian recommendation predictions and the experimental results. It was confirmed numerically and experimentally the influence of the effective bonded length on the ultimate load. In particular:

- if the effective bonded length is lower than the minimum bonded length, the ultimate load increases with the bonded length and the ultimate load depends on both Γ_F and τ_f;
- if the effective bonded length is equal or higher than the minimum bonded length, the ultimate load is no longer affected by the bonded length and it depends only on Γ_F.

Bibliographic references

Aiello M. A., Sciolti S. M. (2006), Analysis of masonry structures strengthened with CFRP sheets, *Construction and Building Materials*, 20:1, 90-100.

Biolzi L., Ghittoni C., Fedele R., Rosati G. (2013), Experimental and theoretical issues in FRP-concrete bonding, *Construction and Building Materials*, 41, 182-190.

Bocciarelli M., Colombi P. (2012), Elasto-plastic debonding strength of tensile steel/CFRP joints, *Engineering Fracture Mechanics*, 85, 59-72.

Ceroni F., Garofano A., Pecce M. (2014), Modelling of the bond behavior of tuff elements externally bonded with FRP sheets, *Composites: Part B*, 59, 248-259.

CNR DT200 (2012), *Istruzioni per la progettazione, l'esecuzione ed il controllo di interventi di consolidamento statico mediante l'utilizzo di compositi fibrorinforzati*. Roma, Italy.

D.M. 20/11/1987, Norme Tecniche per la progettazione, esecuzione e collaudo degli edifici in muratura e per il loro consolidamento (1987). Roma, Italy.

Ferracuti B., Savoia M., Mazzotti C. (2007), Interface law for FRP-concrete delamination, *Composites Structures*, 80:4, 523-531.

Ghiassi B., Marcari G., Oliveira D. V., Lourenço P. B., Numerical analysis of the bond behavior between masonry bricks and composite materials, *Engineering Structures*, 43, 210-220.

Grande E., Imbimbo M., Sacco E. (2011), Bond behaviour of CFRP laminates glued on clay bricks: Experimental and numerical study, *Composites: Part B*, 42:2, 330-340.

Lu X. Z., Teng J. G., Ye L. P., Jiang J. J. (2005), Bond-slip models for FRP sheet/plates bonded to concrete, *Engineering Structures*, 27:6, 920-937.

Monti G., Renzelli M., Luciani P. (2003), FRP adhesion in uncracked and cracked concrete zones, *Proc., 6th International Symposium on FRP Reinforcement for Concrete Structures*. Singapore, 183-192.

Nakaba M., Toshiyuki K., Tomoki F., Hiroyuki Y. (2001), Bond behavior between fiber-reinforced polymer laminates and concrete, *ACI Structural Journal*, 98:3, 359-367.

Ortiz M., Pandolfi A. (1999), Finite-deformation irreversible cohesive elements for three dimensional crack-propagation analysis, *International Journal of Numerical Methods in Engineering*, 44:9, 1267-1282.

Panizza M., Garbin E., Valluzzi M. R., Modena C. (2008), Bond behavior of CFRP laminates on brick masonry. In *Proc., Structural Analysis of Historical Constructions*, D'Ayala D., Fodde E. (ed.), Vol. 2 CRC Press, Boca Raton, FL, 763-770.

Fig. 1 - Test pattern setup for the single shear test.

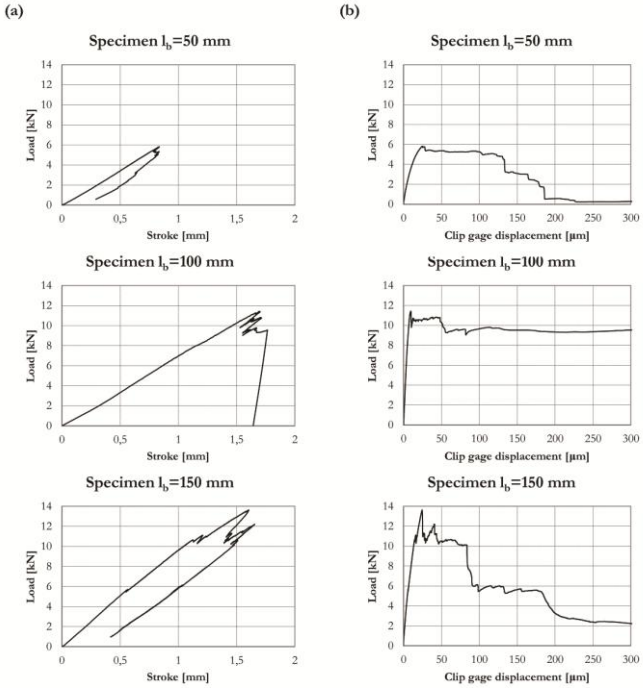

Fig. 2 - Load-stroke displacement curves (a) and load-clip gages displacement curves (b) for different bonded lengths.

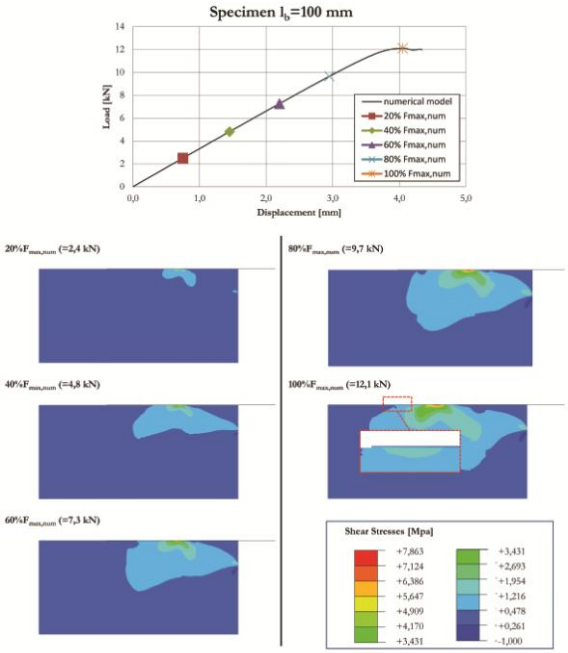

Fig. 3 - Propagation of the shear stress in the support for different load levels. 100 mm bonded length.

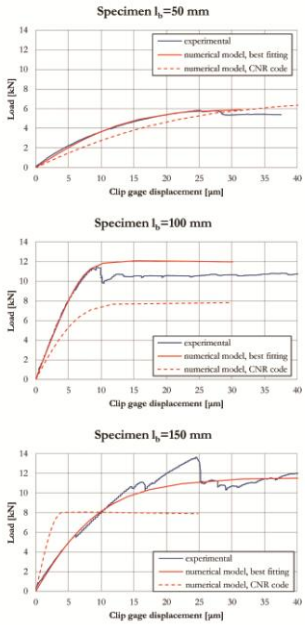

Fig. 4 - Load-clip gages displacement curves for different bonded lengths. Comparison between experimental and numerical results.